Low-Density Lipoprotein Has an Enormous Capacity To Bind (*E*)-4-Hydroxynon-2-enal (HNE): Detection and Characterization of Lysyl and Histidyl Adducts Containing Multiple Molecules of HNE

Suresh P. Annangudi,[†] Yijun Deng,[†] Xiaorong Gu,[‡] Wujuan Zhang,[†] John W. Crabb,[†,‡] and Robert G. Salomon*[,†]

Department of Chemistry, Case Western Reserve University, Cleveland, Ohio 44106-7078, and The Cole Eye Institute, The Cleveland Clinic Foundation, Cleveland, Ohio 44195

Received January 20, 2008

(*E*)-4-Hydroxynon-2-enal (HNE), an electrophilic bifunctional cytotoxic lipid peroxidation product, forms covalent adducts with nucleophilic side chains of amino acid residues. HNE-derived adducts have been implicated in many pathophysiological processes including atherosclerosis, diabetes, and Alzheimer's disease. Tritium- and deuterium-labeled HNE (d_4-HNE) were used orthogonally to study adduction with proteins and individual nucleophilic groups of histidyl, lysyl, and cysteine residues. Using tritium-labeled HNE, we detected the binding of 486 molecules of HNE per low-density lipoprotein (LDL) particle, significantly more than the total number of all reactive nucleophiles in the LDL particle. This suggests the formation of adducts that incorporate multiple molecules of HNE with some nucleophilic amino acid side chains. We also found that the reaction of a 1:1 mixture of d_4-HNE and d_0-HNE with *N*-acetylhistidine, *N*-acetyl-Gly-Lys-OMe, or *N*-acetyl cysteine generates 1:1, 2:1, and 3:1 adducts, which exhibit unique mass spectral signatures that aid in structural characterization. A domino-like reaction of initial 1:1 HNE Michael adducts of histidyl or lysyl nucleophiles with multiple additional HNE molecules forms 2:1 and 3:1 adducts that were structurally characterized by tandem mass spectrometry.

Introduction

Phospholipids that incorporate arachadonic or linoleic acids have doubly allylic methylene groups that are highly susceptible to hydrogen atom abstraction followed by peroxidation leading to an array of reactive oxidation products (*1*). The staggering number of nucleophilic molecular targets in the intracellular as well as intercellular environment for these highly reactive electrophilic products of lipid oxidative fragmentation form a complicated mixture of products, making it very difficult to identify them and assign molecular structures (*2*). Oxidation of lipids in low-density lipoproptein (LDL)[1] is thought to be the initial step in oxidative modification of LDL, which leads to the formation of foam cells and, consequently, atherogenesis (*3*). Oxidative fragmentation of these polyunsaturated lipids can give rise to several cytotoxic products including several γ-hydroxy-α,β-unsaturated aldehydes, which have been shown to be biologically active (*4*) and can act as ligands for the CD36 receptors in macrophages (*5*). Among these products, (*E*)-4-hydroxynon-2-enal (HNE) has been studied extensively due to its proclivity to form pathological adducts (*6–9*) with nucleophilic amino acid residues of proteins. Modification by HNE has been shown to alter the structure (*10*) and function (*11, 12*) of proteins. Furthermore, HNE is a structurally simple γ-hydroxyalkenal whose adducts with biological nucleophiles are most readily characterized.

Earlier studies suggested that arginine, serine, methionine, or tyrosine only form adducts with HNE under nonphysiological conditions, for example, high alkalinity and temperatures much greater than 37 °C (*13, 14*). Lysine, cysteine, and histidine residues readily form Michael adducts (Scheme 1) (*7*). Michael adducts of the histidine imidazole and cysteine thiol residues are stable (*15*). In contrast, Michael addition of the lysyl ϵ-amino group is readily reversible. The formation of Schiff bases with the lysyl ϵ-amino group is also readily reversible, but upon cyclization followed by dehydration, more stable pyrroles are generated (*16*). HNE-derived pyrrole epitopes have been detected in oxidatively damaged LDL, human blood plasma, and atherosclerotic plaques (*8*).

A previous study on the modification of LDL by HNE showed that there is a steady increase in the amount of HNE bound per mol of LDL with increasing amounts of HNE added (*17*). Also, a previous model study detected the formation of adducts that incorporate two or more molecules of HNE per amine group, from the reaction of equimolar amounts of HNE and primary amines, even under high-dilution conditions (*16*). However, structural characterization of all but a few adducts has been a challenge possibly due to their labile nature. Methods employed previously to identify HNE adducts of proteins or amino acids, using $NaBH_4$ reduction or modification by 3,5-dinitrophenylhydrazine, are harsh and may reflect only a fraction of the adducts formed. Because the detection and characterization of these adducts involved derivatization using strong reducing and/or acidic conditions, only adducts that are stable under these

* To whom correspondence should be addressed. Tel: 216-368-2592. Fax: 216-368-2609. E-mail: rgs@case.edu.

[†] Case Western Reserve University.

[‡] The Cleveland Clinic Foundation.

[1] Abbreviations: AA-PC, arachidonyl phosphatidylcholine; BHT, butylated hydroxytoluene; DPM, disintegrations per minute; DTPA, diethylenetriamine pentaacetic acid; EP, ethanolamine phospholipid; ESI, electrospray ionization; HDL, high-density lipoproteins; HNE, (*E*)-4-hydroxy-2-nonenal; d_4-HNE, [8,8,9,9-$^2H_4$]HNE; HSA, human serum albumin; LA-PC, linoleoyl phosphatidyl choline; LC, liquid chromatography; LDL, low-density lipoprotein; MS, mass spectrometry; PBS, phosphate-buffered saline; PE, phosphatidyl ethanolamine; TOF, time-of-flight; TLC, thin-layer chromatography; TNBS, trinitrobenzenesulfonic acid; TIC, total ion current; SIM, selected ion monitoring.

10.1021/tx8000303 CCC: $40.75
Published on Web 06/21/2008

Scheme 1. Generation of HNE and Amino Acid Michael Adducts from Polyunsaturated Fatty Acids

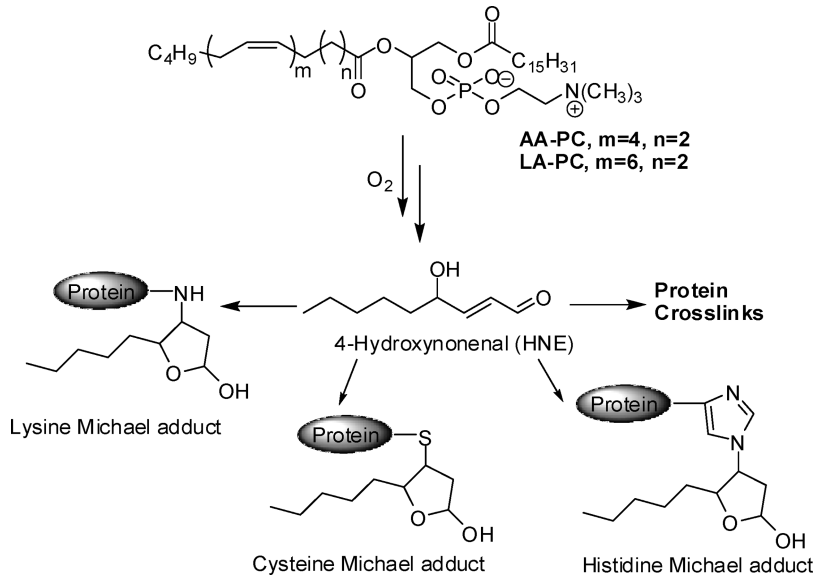

conditions have been detected. There is a need for mild techniques that are compatible with the products, which are stable under physiological conditions but which may readily decompose under harsher conditions. We now report the application of tandem mass spectrometry in conjunction with isotope labeling to probe the adduction chemistry of HNE with LDL and with amino acid residues and to identify the nature of adducts formed under physiomimetic conditions.

Experimental Procedures

General Methods. Liquid scintillation counting was done on a Beckman LS 5801 counter with quench curves made from a Beckman ^{3}H standard set. Samples were prepared with 5 mL of xylene-based scintillation fluid (Fisher Scientific Co., Fairlawn, NJ). UV spectra were obtained with a Perkin-Elmer model Lambda 3B spectrophotometer. Lysine modification was determined by trinitrobenzenesulfonic acid (TNBS) assay (*18*). Spectrapor membrane tubing (M_r cutoff 14000, no. 2) for standard dialysis was obtained from Fisher Scientific Co. (Pittsburgh, PA). The following commercially available materials were used as received: human serum albumin (HSA, fraction V) and disodium *p*-nitrophenyl phosphate was from Sigma (St. Louis, MO). Phosphate-buffered saline (PBS) was prepared from a pH 7.4 stock solution containing 0.2 M NaH_2PO_4/Na_2HPO_4, 3.0 M NaCl, and 0.02% NaN_3 (w/w). HNE and tritium-labeled HNE ([9-^{3}H]HNE, 63.5 μCi/mmol) were prepared as described earlier (*19*). Native human LDL (3.8−3.9 mg apoB-100/mL) was isolated as described previously (*20*). Nuclear magnetic resonance (NMR) spectra were recorded on a Varian Gemini spectrometer operating at 200, 300, 400, or 600 MHz. All materials were obtained from Aldrich (Michigan) unless otherwise specified. Thin-layer chromatography (TLC) was performed on glass plates precoated with silica gel (Kieselgel 60 F_{254}, E. Merck, Darmstadt, Germany). R_f values have been quoted for plates of thickness 0.25 mm. The plates were visualized with iodine or phosphomolybdic acid reagent (*21*). Flash column chromatography was performed on 230−400 mesh silica gel supplied by Merck (Darmstadt, Germany). For all reactions performed in an inert atmosphere, argon was used unless specified.

Mass Spectrometry. All high-resolution mass spectra of synthesized compounds were recorded on a Kratos AEI MS25 RFA high-resolution mass spectrometer at 20 eV. Mass spectra of the HNE adducts were analyzed using matrix-assisted laser desorption/ionization time-of-flight (MALDI-TOF) mass spectrometer (Voyager Pro-DE, Applied Biosystems, Foster City, CA) or quadrupole time-of-flight mass (Q-TOF) mass spectrometer (Micromass, Manchester, United Kingdom). Tandem mass analysis of HNE adducts was performed using the Q-TOF mass spectrometer. The samples were infused using a 100 μL Hamilton syringe, using a syringe pump (Harvard apparatus, Pump 11), onto a capillary column (PicoFrit 0.050 mm × 50 mm, 5 μm; New Objective Inc., Woburn, MA) at 0.5 μL/min, which is connected to an in-house-designed electrospray ionization source (ESI). The mass spectrometer was operated in standard MS and MS/MS switching modes. The MS data were collected for the mass range of *m/z* 50−1500, and MS/MS data analyses utilized Micromass software (MassLynx) version 3.5. The instrument was calibrated using a solution of 2 fmol of [Glu1]Fibrinopeptide B (Sigma) in 50% aqueous acetonitrile with 0.1% formic acid. The intensity of the peak from the MS/MS spectrum at 785.4 *m/z* was used as a reference for calibration. The final mass measurement accuracy of ≤10 ppm was achieved before samples were analyzed.

Selected Ion Monitoring. Selected ion monitoring of HNE adducts was performed using a Waters Alliance 2690 HPLC (Waters, Wilmington, DE) coupled to an online Quattro Ultima electrospray mass spectrometer (Micromass, Manchester, United Kingdom). The samples analyzed for selected ion monitoring were chromatographically separated on a reversed phase column and detected in positive mode. The chromatographic separation was achieved using a Prodigy ODS-2, 5 μm column (Phenomenex, United Kingdom, 150 mm × 2.0 mm i.d.), with a binary solvent (water and methanol) gradient. The solvents were supplemented with 0.2% formic acid. The flow rate was 200 μL/min.

TNBS Assay for Protein Lysine Modification. The following solutions were prepared for determining HNE-modified lysyl residues in LDL by the TNBS assay: solution A, freshly prepared 0.1 M Na_2SO_3; solution B, 0.1 M NaH_2PO_4; solution C, 0.1 M $Na_2B_2O_7{\cdot}10H_2O$ in 0.1 M NaOH; solution D, 1.5 mL of solution A + 98.5 mL of solution B; and solution E, freshly prepared 5% aqueous TNBS solution. LDL (0.5 mg/mL) was treated with tritium-labeled HNE (2.0 mM, or final concentra-

tion, 0.2 mM) at 37 °C in PBS buffer (10 mM, pH 7.4) in the presence of diethylenetriamine pentaacetic acid (DTPA, 100 μM) and butylated hydroxytoluene (BHT, 40 μM). Aliquots were removed at various time intervals. The lysyl modification by HNE was determined by the following procedure. The aliquot of LDL-HNE mixture (100 μL) was combined with water (400 μL) and mixed with 500 μL of solution C in a 5 mL glass tube. To this mixture, solution E (20 μL) was added, and the resulting mixture was incubated at room temperature for 30 min in the dark. Then, 2 mL of solution D was added to each sample, and the absorbance was measured twice at 420 nm. The mean absorbance values were used for calculating available primary amino residues in LDL and estimating % of reactive lysyl groups modified by HNE relative to the native LDL ($\epsilon_{max} = 1.92 \times 10^4$ M^{-1} cm^{-1} is the molar extinction coefficient of TNP-lys at 420 nm). Because phosphatidyl ethanolamine can also rapidly react with TNBS, the modification of amino residues determined by the TNBS assay also includes modification of ethanolamine phospholipids (EPs) in LDL.

Binding to LDL with Various Initial Concentrations of HNE. LDL (0.5 mg/mL) was exposed to different initial concentrations (0.05, 0.1, 0.2, 0.4, 0.8, and 1.6 mM) of tritium-labeled HNE (63.5 μCi/mmol) for 24 h at 37 °C in PBS buffer (10 mM, pH 7.4) in the presence of DTPA (100 μM, final concentration) and BHT (40 μM, final concentration), followed by dialysis for 24 h to remove unbound HNE. A tritium-labeled HNE solution (1 mg/mL in ethyl acetate) was freshly prepared for making the above serial HNE solutions. The concentration of the stock HNE solution (1 mg/mL) was determined by measurement of UV absorbance at 224 nm presuming a molar extinction coefficient of 13750 M^{-1} for HNE in MeOH and confirmed by quantitative radiochemical analysis. The radioactivity of HNE bound to LDL was determined in disintegrations per minute (DPM) by liquid scintillation counting. The DPM was converted to μCi by dividing by 2.2×10^6 (DPM/μCi). The amount of HNE bound to LDL was calculated by using the specific radioactivity (63.5 μCi/mmol) for the tritium-labeled HNE.

Time Dependence for Adduction of Tritiated HNE to LDL or HSA. LDL (0.5 mg/mL, 0.97 μM, MW = 515000, 350 lys/LDL) and HSA (0.38 mg/mL, 5.7 μM, MW = 66437, 59 lys/LDL), which contain the same level of lysyl residues, were exposed, respectively, to two different initial concentrations (0.2 and 2.0 mM in 10 mM PBS solution) of tritium-labeled HNE (63.5 μCi/mmol) at 37 °C for 48 h. Aliquots were removed at various time intervals, followed by dialysis against PBS buffer (10 mM) with ethylenediamine tetraacetate (1 mg/mL) for 24 h to remove unbound HNE. DTPA (100 μM) and BHT (40 μM) were added to the HNE-LDL samples to avoid autoxidation of LDL during the incubation and storage. The radioactivity of HNE bound to the LDL or HSA was determined by liquid scintillation counting in DPM. The DPM was converted to μCi by dividing by 2.2×10^6 (DPM/μCi). The amount of HNE bound to proteins was calculated from the specific radioactivity (63.5 μCi/mmol) of the HNE.

Synthesis of [8,8,9,9-$^2H_4$]HNE (d_4-HNE). Toluene-4-sulfonic Acid Pent-4-ynyl Ester (2). A suspension of *p*-tosyl chloride (3.4 g, 17.9 mmol) and triethylamine (6 mL) in CH_2Cl_2 (25 mL) was added dropwise to pent-4-yn-1-ol (1 g, 11.9 mmol) at 0 °C, and the reaction mixured was stirred at 0 °C. When TLC showed no starting material, the reaction mixture was extracted with ethyl ether (3 × 20 mL). The extract was washed with saturated sodium bicarbonate, water, and brine. After it was dried over $MgSO_4$, the solvent was removed in vacuo and purified by column chromatography with 5% ethyl acetate in petroleum ether ($R_f = 0.7$) to yield a oily liquid **2** (2.43 g, 86%) (*22*).

[4,4,5,5-$^2H_4$]Toluene-4-sulfonic Acid Pent-4-nyl Ester (3). To a flask containing benzene (2 mL) flushed with argon was added freshly prepared Wilkinson's catalyst $RhCl(PPh_3)_3$ (12 mg, 12.9 μmol) (*23*). The flask was flushed with argon for 5 min, and the valve turned to deuterium gas. The color of the solution turned ice-tea brown. After 5 min, a solution of **2** (336 mg, 1.41 mmol) in degassed benzene (1 mL) was added dropwise. The reaction was allowed to proceed under a positive pressure of D_2 until the reaction ceased to consume D_2. The solvent was removed on a rotatory evaporator. The product was extracted by trituration with hexanes (3 × 20 mL) and purified by column chromatography with 5% ethyl acetate in hexanes ($R_f = 0.5$) to yield an oily liquid **3** (260 mg, 74%). ^{1}H NMR (CD_3Cl, 300 MHz): δ 7.77 (d, $J_1 = 6.2$ Hz, $J_2 = 1.6$ Hz, 2H), 7.33 (d, $J = 8.4$ Hz, 2H), 4.02 (t, $J = 6.5$ Hz, 2H), 2.45 (s, 3H), 1.63−1.64 (2H), 1.26 (t, $J = 7.2$ Hz, 2H), 0.8031 (bs, 1H). ^{13}C NMR (CD_3Cl, 75 MHz): δ 144.8, 133.4, 129.9, 128.0, 70.9, 28.6, 27.3, 21.8, 21.1(t), 13.3(q). HRMS (EI) *m/z* calcd for $C_{12}H_{14}D_4O_3S^+$ (M^+), 246.1224; found, 247.1292 $(M + H)^+$ (*24*).

[7,7,8,8-$^2H_4$]-1-(2,2-Dimethyl-[1,3]dioxolan-4-yl)oct-1-en-3-ol (6). To a stirred solution of sodium iodide (750 mg, 5 mmol) in freshly distilled acetone (15 mL) was added potassium carbonate (550 mg, 4 mmol) and tosylate **3** (500 mg, 2 mmol). The solution was refluxed for 3 h or until the reaction was complete. The solvent was removed on a rotatory evaporator and then on a vacuum pump to give crude iodide **4**. This product was used for the next step without further purification. ^{2}H NMR ($CDCl_3$, 90 MHz): δ 1.185, 1.120, 0.884, 0.737. ^{1}H NMR ($CDCl_3$, 300 MHz): δ 3.19 (t, $J = 7$ Hz, 2H), 1.78−1.83 (m, 2H), 1.36 (t, $J = 7.7$ Hz, 2H), 0.86 (s, 1H).

A solution of *t*-butyl lithium (6 mmol) in hexanes was added dropwise to a stirred solution of iodide **4** (∼150 mg, 0.74 mmol) in freshly distilled ethyl ether:pentane (2:1, 15 mL) at −78 °C under argon. After 10 min at −78 °C, the reaction mixture was allowed to warm to room temperature to generate the alkyl lithium. The reaction mixture was then cooled to −78 °C, and 3-(2,2-dimethyl-[1,3]dioxolan-4-yl)-propenal (**5**) (*25*) (108 mg, 0.7 mmol) was added dropwise with stirring over for 5 min. After the resulting mixture was stirred for 30 min, saturated NH_4Cl was added. The resulting mixture was extracted with ethyl ether (3 × 15 mL). The organic extract was washed with brine, and solvent was removed on a rotatory evaporator. The crude product was purified on a flash column with 25% ethyl acetate in hexanes to deliver **6** (136 mg, 84%). ^{1}HNMR ($CDCl_3$, 300 MHz): δ 5.82 (dd, $J = 15.4$, 6.1 Hz, 1H), 5.64 (ddd, $J = 16.5$, 7.4, 2.3 Hz, 1H), 4.5 (dd, $J = 13.7$, 7.1 Hz, 1H), 4.06−4.13 (m, 2H), 3.57 and 3.58 (2t, $J = 7.9$ Hz, $J = 7.7$ Hz, 1H), 1.25−1.60 (8H), 1.40 (s, 3H), 1.37 (s, 3H), 0.82 (s, 1H). ^{13}C NMR ($CDCl_3$, 300 MHz): δ 137.46, 137.39, 127.81, 127.76, 109.40, 109.38, 76.57, 72.04, 71.98, 69.49, 69.47, 37.15, 37.05, 31.48, 26.71, 25.92, 25.05, 24.99, 21.62(q), 13.23 (q). HRMS *m/z* calcd $C_{13}H_{20}D_4O_3$ 232.1972 $(M)^+$ found, 233.2035 $(M + H)^+$; 231.1872, $(M - H)^+$.

[8,8,9,9-$^2H_4$]-4-Hydroxy-2(*Z*)-nonenal (7). This product was accessed by two different methods.

Method A. A suspension of sodium periodate (24 mg, 0.117 mmol) in acetic acid/water (2:1, v/v, 2 mL) was added to compound **6** (13 mg, 0.056 mmol), and the mixture was stirred magnetically for 4 h at 40 °C or until the reaction was complete. Then, the solvent was removed by rotary evaporation under

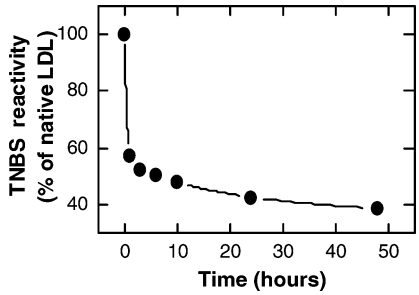

Figure 1. Time course for the change in TNBS reactivity of LDL (0.50 mg/mL) upon incubation with tritium-labeled HNE (2.0 mM) at 37 °C for up to 48 h.

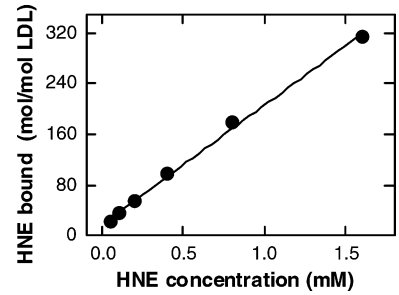

Figure 2. Correlation of HNE bound to LDL (0.5 mg/mL, 0.97 μM) with varying initial HNE concentrations after 24 h of incubation at 37 °C.

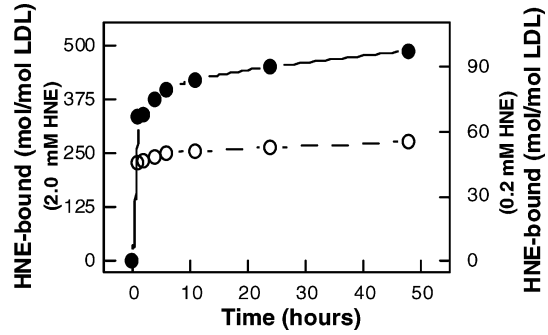

Figure 3. Time course for binding of HNE with LDL (0.50 mg/mL) as a function of initial HNE concentration: LDL-HNE (2.0 mM) (solid circles) and LDL-HNE (0.2 mM) (open circles).

reduced pressure. The last traces of HOAc were removed by azeotropic distillation with *n*-heptane (3:1 mL) under high vacuum. The resulting residue was flashed chromatographed on a silica gel column (30% ethyl actetate in hexanes) to give **7** (8 mg, 89%).

Method B. A solution of the compound **6** (13 mg, 0.056 mmol) in acetic acid/water (2:1, v/v, 1.2 mL) was stirred magnetically for 4 h at 40 °C. Then, the solvent was removed by rotary evaporation under reduced pressure. The last traces of HOAc were removed by azeotropic distillation with *n*-heptane (3:1 mL) under high vacuum. Dry methylene chloride (2 mL) and Na_2CO_3 (5.7 mg, 0.054 mmol) were added to the residue. The solution was stirred magnetically at −78 °C under an argon atmosphere, and $Pb(OAc)_4$ (31 mg, 0.07 mmol) was added. The resulting solution was stirred for 30 min. The solvent was then removed, and the residue was flashed chromatographed on a silica gel column (30% ethyl actetate in hexanes) to give **7** (7 mg, 78%). ^{1}H NMR (CD_3Cl, 300 MHz): δ 9.57 (d, J = 7.7 Hz, 1H), 6.80 (dd, J_1 = 15.7 Hz, J_2 = 4.5 Hz, 1H), 6.29 (dd, J_1 = 15.7 Hz, J_2 = 7.7 Hz, 1H), 4.02 (t, J = 6.5 Hz, 2H), 2.45 (s, 3H), 1.63−1.64 (2H), 1.26 (t, J = 7.2 Hz, 2H), 0.8031 (bs, 1H). ^{13}C NMR (CD_3Cl, 75 MHz): δ 193.1, 158.7, 130.6, 92.3, 71.1, 36.5, 31.3, 29.2, 24.8.

Synthesis of HNE Adducts of *N*-Acyl Amino Acids. A solution of [8,8,9,9-$^2H_4$]HNE (d_4-HNE) (5 mM in ethyl acetate) was freshly prepared and added to a solution of unlabeled HNE (5 mM in ethyl acetate) to make a 1:1 stock solution. The concentrations of the stock solutions were determined by measurement of UV absorbance at 224 nm presuming a molar extinction coefficient of 13750 M^{-1} for HNE in MeOH (*26*). To a 1.5 mL glass vial was added a 1 mL stock solution of HNE (d_4:d_0), and the solvent was evaporated using a gentle stream of N_2 gas. In a typical reaction, a solution of *N*-acyl amino acid, for example, α-*N*-acetyl-lysine (20 μM), in PBS (10 mM, pH 7.4) was then added to the d_4-HNE and HNE (1:1) to give 10 μM final concentration of total HNE. The mixture was incubated at 37 °C for 24 h. Longer reaction times were required, in some cases, to favor the formation of adducts that are generated in low abundances, for example, 36−48 h at room temperature for 3:1 HNE: *N*-acetyl-glycine-lysine-OMe adducts. Following the incubation, an aliquot of the reaction mixture was quickly dried using a high-speed vacuum evaporator and then stored at −20 °C until analysis by Q-TOF mass spectrometer.

Results

Decrease of TNBS Reactivity of LDL upon Incubation with HNE. We found a significant decrease (62%) of TNBS reactivity in LDL (0.50 mg/mL) that was incubated with tritium-labeled HNE (2.0 mM) at 37 °C for 48 h (Figure 1). This corresponds to the loss of 165 (based on ϵ_{max} = 19200 L mol^{-1} cm^{-1}) (*27*) or 230 (based on ϵ_{max} = 14600 L mol^{-1} cm^{-1}) (*28*) primary amino residues per LDL particle. In comparison, oxidation of LDL, by exposure to 5 μM $CuSO_4$ at 37 °C for 20 h, was previously shown to result in the loss of 130−145 "lysyl residues" per LDL based on TNBS assay (*29, 30*). We find that the TNBS reactivity of LDL decreases rapidly in the first hour in the reaction of LDL with HNE. Thus, up to 70% of total HNE binding occurs in the first hour.

Dependence of HNE Binding to LDL on HNE Concentration. HNE binding to LDL was determined by quantitative radiochemical analysis with tritium-labeled HNE. LDL (0.50 mg/mL, 0.97 μM) was exposed to different initial concentrations of tritium-labeled HNE for 24 h at 37 °C in PBS buffer (10 mM, pH 7.4) in the presence of DTPA and BHT to prevent autoxidation, followed by dialysis for 24 h to remove unbound HNE. After 24 h of incubation, up to 314 HNE molecules bind to an LDL particle with 1.6 mM HNE initial concentration, and the amount of HNE bound to LDL increased linearly with initial HNE concentration (Figure 2). Upon the incubation of LDL (0.50 mg/mL, 0.97 μM) with tritium-labeled HNE (2.0 mM, instead of 1.6 mM) for 48 h, rather than 24 h, at 37 °C in PBS buffer (10 mM, pH 7.4) in the presence of DTPA and BHT, 486 HNE molecules bound per LDL particle.

Time Course of HNE Binding to LDL or HSA. Solutions containing the "same level" of lysyl groups in either LDL (0.5 mg/mL, 0.97 μM) or HSA (0.38 mg/mL, 5.7 μM) in PBS (10 mM, pH 7.4) were treated with two initial concentrations of tritium-labeled HNE (0.2 or 2.0 mM) for 24 h at 37 °C in PBS buffer (10 mM, pH 7.4), followed by dialysis against PBS (10 mM) for 24 h to remove unbound HNE. DTPA and BHT were added to the LDL solution to avoid autoxidation of LDL during the incubation and storage. The time course of HNE binding to LDL is shown in Figure 3. Binding of HNE to LDL occurs in two phases: an initial "rapid phase" corresponding to more than 80% of total HNE binding within 3 h (about 70% of total binding HNE occurs in the first hour) and a "slower second

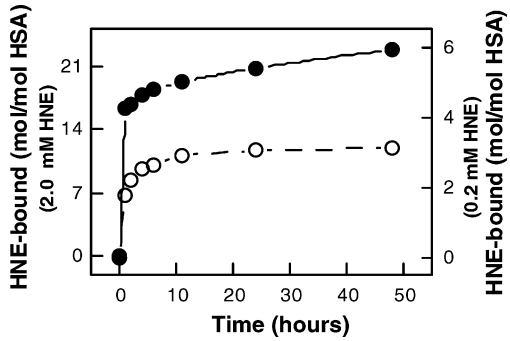

Figure 4. Time course for binding of HNE with HSA (0.38 mg/mL) as a function of initial HNE concentration: HSA-HNE (2.0 mM) (solid circles) and HSA-HNE (0.2 mM) (open circles).

Scheme 2. Synthesis of [7,7,8,8-$^2H_4$]HNE (7)

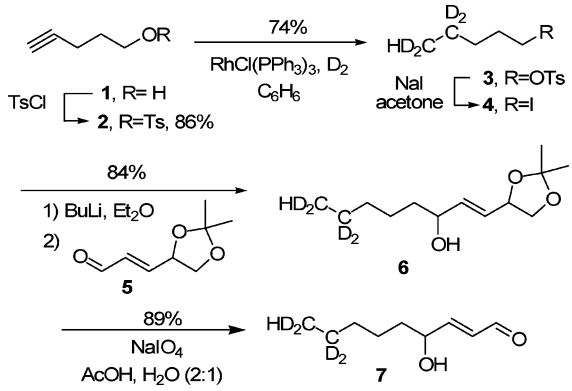

phase" corresponding to about 20% of total binding during an additional 45 h. To determine whether this behavior is a characteristic of lipoprotein particles or is a general characteristic of the reaction of HNE with nucleophiles, for example, in protein side chains, we examined the time course of HNE binding to HSA. Binding of HNE to HSA also occurs in two phases (Figure 4). This result is consistent with earlier reports using ^{13}C NMR spectroscopy (*31*).

Synthesis of d_4-HNE. 4-Pentynol (**1**) was used as a precursor for carbons 5−9 and the protected aldehyde **5** as the precursor for carbons 1−4 of the d_4-HNE (Scheme 2). The tosyl ester **3** of d_4-pentanol was obtained in 74% yield by deuteration of pent-4-ynyl tosyl ester (**2**) (*22*) using Wilkinson's catalyst, RhCl(P-$Ph_3)_4$, and deuterium (*24*). An intermediate [4,4,5,5-$^2H_4$]pentyl iodide (**4**) was generated by heating the tosylate **3** with NaI and K_2CO_3 in refluxing acetone (Scheme 3) (*32*). The iodide **4** was converted into [4,4,5,5-$^2H_4$]pentyllithium by metal halogen exchange of with *t*-BuLi. Alkylation of aldehyde **5** by the pentyllithium yielded the stable precursor **6** of d_4-HNE in 84% overall yield. Preparation of HNE from this precursor was performed by a one-step procedure, using $NaIO_4$ and aqueous acetic acid, to give d_4-HNE (**7**) in 89% yield. An alternative two-step procedure using acetic acid and lead tetraacetate gave HNE in 78% yield (*19*).

Mass Spectrometric Analysis of HNE Adducts. The MALDI-TOF mass spectra of product mixtures generated in the reactions of HNE (d_4:d_0, 1:1) with *N*-acetyl histidine, *N*-acetyl cysteine, or *N*-acetyl-glycine-lysine methyl ester exhibited multiple peaks that correspond to d_0, d_4, and d_8 isotopologues (chemical species that differ only in isotopic composition) that appear as unique sets of "multiplets" with a mass difference of 4 Da (for a detailed explanation of the principles involved, see the Supporting Information, pp S2−S4). Further analysis was performed using a Q-TOF mass spectrometer by single (Figure 5) and tandem MS modes to identify the products formed. Also, semiquantitative analyses of various molecular ions were done by liquid chromatography and selected ion monitoring [LC-ESI/selected ion monitoring (SIM)/MS] using a Quattro Ultima (Micromass, Manchester, United Kingdom) mass spectrometer.

HNE Adducts of *N*-Acetyl-histidine. The parent ion for the Michael adduct (see Scheme 1) of *N*-acetyl-histidine with HNE (d_4:d_0, 1:1) appears as a "doublet" at *m*/*z* 354 and 358 (Figure 5C). Tandem MS/MS analysis of these ions resulted in a specific signature of fragments corresponding to the labeled or unlabeled HNE. Thus, MS/MS of the *m*/*z* 354 ion yields daughter ions at *m*/*z* 336, 312, 308, 266, 198, 180, 177, 156, 152, 139, 110, and 95, while tandem MS/MS of the ion at *m*/*z* 358 yields daughter ions at *m*/*z* 340, 316, 312, 270, 198, 180, 177, 156, 152, 143, 110, and 95 (see the Supporting Information, Figure S1). On the basis of mass differences between the ions from both of the spectra, daughter ions containing the C5−C9 alkyl chain of the HNE were identified. The structures of the ions in this mass spectrum can be rationalized based on the patterns observed in the fragmentation of *N*-acetyl-histidine. Similar to the fragmentation pattern reported for *N*-acetyl-histidine (*35*), fragmentation of the Michael adduct exhibits peaks originating from loss of a ketene [$MH^+ - (CH_2{=}CO)$] (*m*/*z* 312) from the *N*-acetyl group and carboxyl loss [$MH^+ - CO - H_2O$)] (*m*/*z* 308) from C-terminal acid. Additionally, the *m*/*z* 312 and 308 undergo a subsequent loss of the carboxyl or the ketene group, respectively, to generate peaks at *m*/*z* 266. The daughter ion at *m*/*z* 139 (and *m*/*z* 143 from the d_4-HNE) is derived from the HNE moiety possibly through loss of H_2O of the protonated hemiacetal product from retro Michael cleavage of the adduct (*33–36*).

A 2:1 HNE Adduct with *N*-Acetyl-histidine. The combined mass spectra from the total ion chromatogram of the reaction product mixture (Figure 5) also showed ions with *m*/*z* much greater than 400. These molecular ion peaks can only be formed by reaction of two or more of the reaction components. A "triplet" (see the Supporting Information, pp S2−S4, for an explanation of this concept) was observed at *m*/*z* 510, 514, and 518 (1:2:1) that would correspond to an adduct with two molecules of HNE and one of *N*-acetyl-histidine. The tandem MS/MS of the *m*/*z* 510 precursor ion generates some of the prominent fragments corresponding to the loss of carboxyl, acetyl, and d_0-HNE at *m*/*z* 464, 468, and 354, respectively (Figure 6C), including ions observed for the fragmentation of the *m*/*z* 354 ion. Fragmentation of the parent ions at *m*/*z* 514 and 518 generated daughter ions with masses 4 or 8 Da more than those observed for the *m*/*z* 510 ion (Figure 6A,B).

Two structures for the 2:1 adduct are chemically logical. They are a Michael-aldol adduct **8** or a Michael-Michael adduct **10** (both shown protonated in Scheme 3). Each of these will undoubtedly exist in equilibrium with a plethora of multicyclic hemiacetal forms analogous to that shown in Scheme 1 for the 1:1 adduct. The fragments **11** and **12** could be produced from either **8** or **10** by McLafferty rearrangements (Figure 6). Thus, the peak at *m*/*z* 466 (from MS/MS of *m*/*z* 510) can be generated either from the cleavage of "bond c" through McLaffety rearrangement of **10** or by loss of a carboxyl group ($MH^+ - CO - H_2O$) from **8** as shown in Scheme **3**. However, the peak at *m*/*z* 422 can only be formed by loss of carboxyl group ($MH^+ - CO - H_2O$) from **13**, suggesting that this fragment ion is derived from **10** and not from **8**. Furthermore, if **15** were derived from **8**, the formation of a fragment ion at *m*/*z* 424, which corresponds to ketene loss from **15**, is expected but is not observed. Therefore, the 2:1 adduct is assigned the structure **10** rather than **8**.

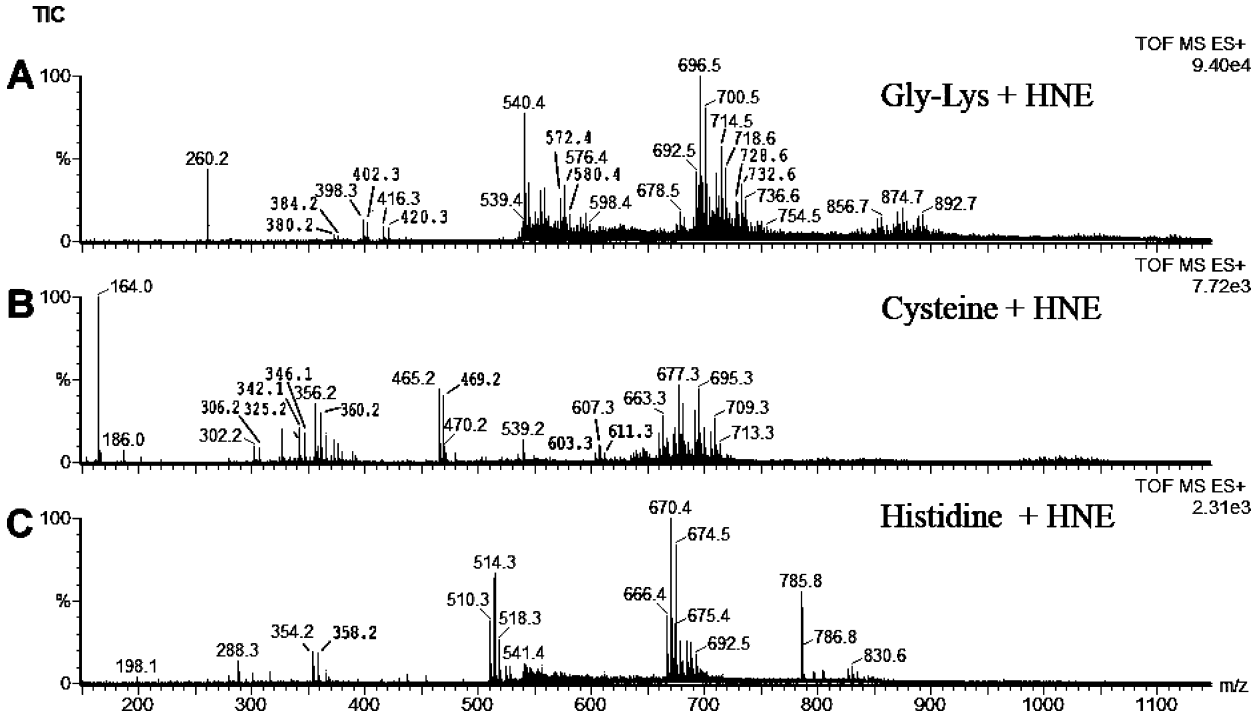

Figure 5. ESI-TOF-MS of reaction product mixtures generated from HNE (d_4:d_0, 1:1) and (A) *N*-acetyl-glycyl-lysine-OMe, (B) *N*-acetyl cysteine, and (C) *N*-acetyl-histidine.

Scheme 3. Structural Characterization of the 2:1 HNE-*N*-Acetylhistidine Adduct by MS/MS Analysis

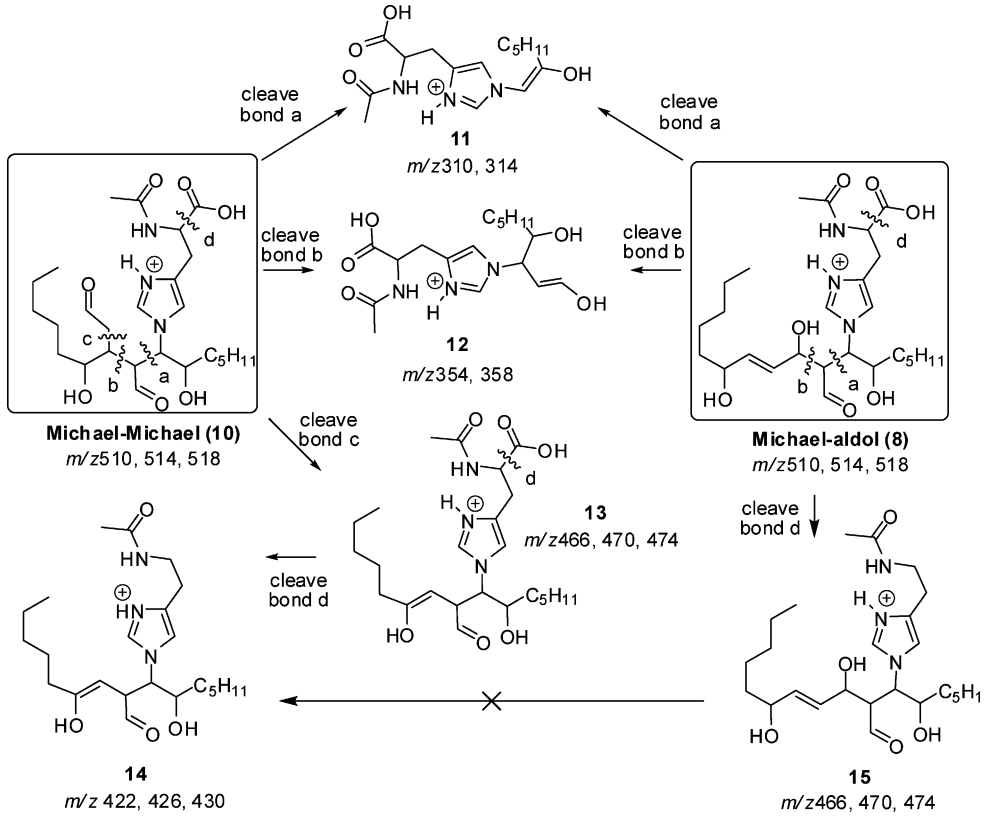

A 3:1 HNE Adduct with *N*-Acetyl-histidine. A "quadruplet" (see the Supporting Information, pp S2−S4, for an explanation of this concept) of ions at *m*/*z* 666, 670, 674, and 678 in an approximate 1:3:3:1 distribution is present in the ESI-MS of the reaction product mixture (Figure 5C) representing adduction of three molecules of HNE with one of *N*-acetyl-histidine. Tandem MS/MS analysis of the *m*/*z* 666 (see the Supporting Information) ion yielded daughter ions at *m*/*z* 622, 578, and 510 as well as daughter ions that were observed in the fragmentation of *m*/*z* 510 ions (Figure 6), and fragmentation of the *m*/*z* 670, 674, and 678 parent ions gave corresponding daughter ions 4 or 8 Da heavier than those observed for the *m*/*z* 666 ion.

HPLC separation of the product mixture from reaction HNE with *N*-acetyl-histidine was monitored on a Quattro Ultima electrospray mass spectrometer (Micromass) by LC-ESI/SIM/

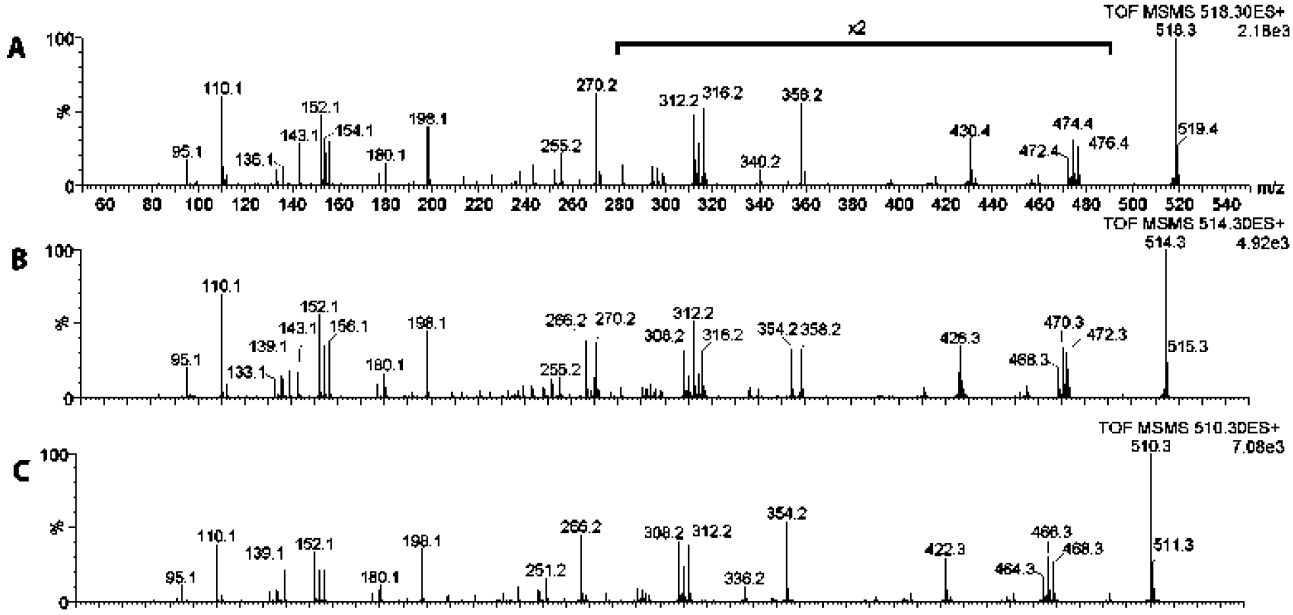

Figure 6. ESI-TOF-MS/MS of molecular ions at (A) *m/z* 518, (B) *m/z* 514, and (C) *m/z* 510 from infusion of the reaction product mixture from HNE (d_4:d_0, 1:1) and *N*-acetyl histidine. *m/z* ranges marked with an "x2" are magnified two times in the *y*-axis.

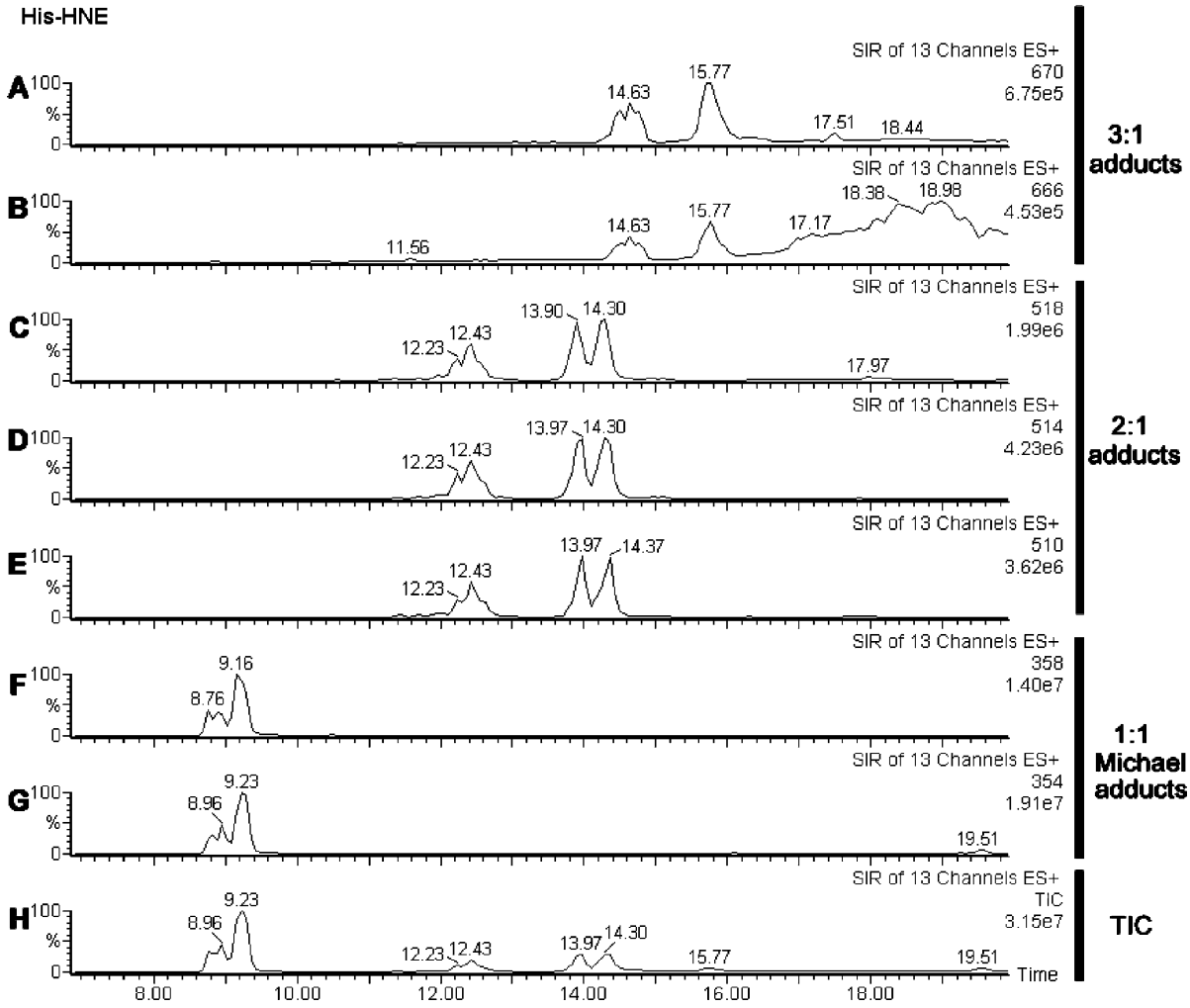

Figure 7. LC-ESI/SIM/MS for the reaction product mixture from *N*-acetyl histidine and HNE (d_4:d_0, 1:1) monitored for the masses (A) *m/z* 670, (B) *m/z* 666, (C) *m/z* 518, (D) *m/z* 514, (E) *m/z* 510, (F) *m/z* 358, (G) *m/z* 354, and (H) the total ion chromatogram.

MS of the prominent ions mentioned above. As evident from the chromatograms in Figure 7, the peaks derived from each adduct and its d_4-labeled isomer have similar signatures. The 1:1 Michael adduct is expected to be comprised of four diastereomers that emerge at 8.6−9.4 min. In the case of 2:1 and 3:1 HNE/*N*-acetyl histidine adducts, much more complex mixtures of diastereomers are anticipated. The total ion current (TIC) for 1:1 adducts is greater than for 2:1 adducts, and that

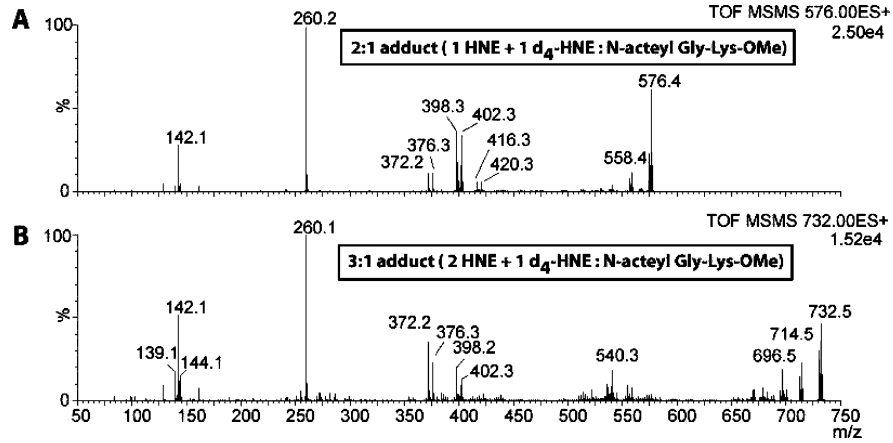

Figure 8. ESI-TOF-MS/MS analysis of molecular ions corresponding to 2:1 adduct with one HNE, one d_4-HNE and one *N*-acetyl-Gly-Lys-OMe (A) *m*/*z* 576 and 3:1 adduct corresponding to two HNE, one d_4-HNE and one *N*-acetyl-Gly-Lys-OMe (B) *m*/*z* 728. For MS/MS corresponding to other 2:1 and 3:1 adducts, see the Supporting Information.

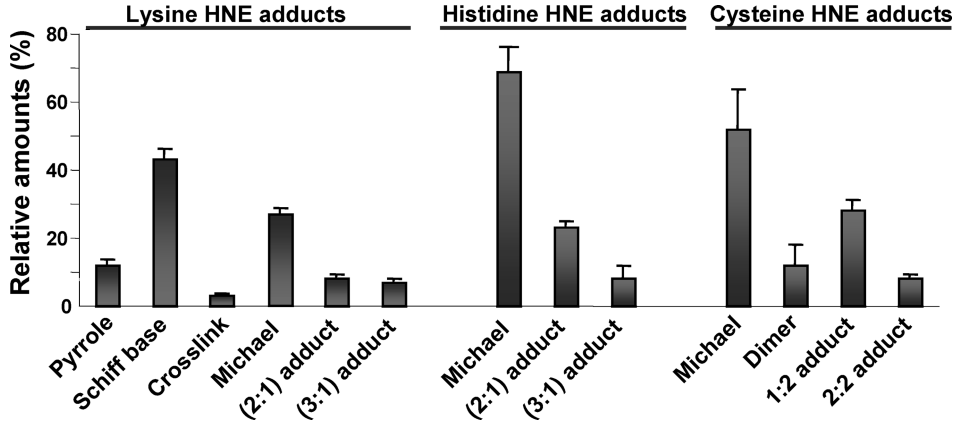

Figure 9. Relative amounts of adducts formed by reaction of HNE with *N*-acetyl-Gly-Lys-OMe, *N*-acteyl-histidine, and *N*-acetyl cysteine calculated using LC-ESI/SIM/MS. The vertical scale reflects the percentage of the each adduct present in the reaction mixture (with respect to the adducts selectively monitored). Values are averages of two independent experiments, and the error bars indicate the range. Cross-link, lysine:HNE (2:1) adducts.

for 3:1 adducts is relatively minor. Also, with the increase in the number of HNE molecules adducted on to *N*-acetyl-His, the polarity of the adducts decrease dramatically (1:1 > 2:1 > 3:1).

HNE Adducts of *N*-Acetyl-glycyl-lysine Methyl Ester. *N*-Acetyl-glycyl-lysine methyl ester (*N*-acetyl-Gly-Lys-OMe) was used to explore the adduction pattern with HNE of the ϵ-amino group of lysyl residues. The product mixture from the reaction of HNE (d_4:d_0, 1:1) with *N*-acetyl-Gly-Lys-OMe was analyzed by ESI-TOF-MS to determine the nature of these adducts. The tandem MS/MS spectrum of the molecular ion at *m*/*z* 416 and the isotope-labeled peak at *m*/*z* 420 correspond to the Michael (1:1) adduct (see Scheme 1) based on the molecular weight and pattern of fragmentation (see the Supporting Information, Figure S5) (*37*). The major peaks in the MS/MS are formed from the loss of water (−18), an acetyl group (−44), and by retro-Michael elimination (−156). Molecular ions corresponding to a Schiff base adduct of HNE with *N*-acetyl-glycine lysine methyl ester were observed at *m*/*z* 398 and 402 (see the Supporting Information, Figure S6). The tandem MS/MS of molecular ions at *m*/*z* 380 and *m*/*z* 384, corresponding to a pyrrole adduct of the HNE (d_4:d_0, 1:1) with lysine, show a fragmentation consistent with the structure of these adducts (see the Supporting Information, Figure S7). One prominent feature among these spectra is the absence of the retro-Michael adduct fragment at *m*/*z* 139/143 in the MS/MS of both the Schiff base and the pyrrole adducts (see the Supporting Information, Figure S7 and Scheme S1).

Ions that correspond to more than one HNE adducted to *N*-acetyl-Gly-Lys-OMe were also observed. The ESI-TOF-MS showed ions at *m*/*z* 572, 576, and 580 and *m*/*z* 728, 732, 736, and 740 along with the fragments derived from dehydration of these adducts (Figure 5A). The ESI-TOF-MS/MS of these molecular ions generated prominent daughter ions from the loss of water and HNE. MS/MS spectra corresponding to 2:1 adducts with *m*/*z* 572, 576, and 580 (corresponding to M, M + 4, and M + 8) and those of 3:1 [HNE:(*N*-acetyl-Gly-Lys-OMe)] adducts at with *m*/*z* 728, 732, 736, and 740 (corresponding to M, M + 4, M + 8, and M + 12) are shown in Figure 8 (also see the Supporting Information, Figures S6 and S7).

Similar to the multiple HNE adducts of histidine, the fragmentations of both the 3:1 and the 2:1 adducts **17** and **18** of HNE with *N*-acetyl-glycine lysine methyl ester can possibly be explained by McLafferty rearrangements (see the Supporting Information, Scheme 4) of parent ion structures corresponding to two and three consecutive Michael additions, respectively. Nevertheless, unambiguous structural assignment for these adducts requires additional experiments, which are beyond the scope of the present study.

Several peaks resulting from loss of multiple H_2O (−18) are also observed in the MS/MS spectra. This is a prominent feature of these adducts. The intense peaks resulting from loss of water from the lysine Michael adducts contrast with the relatively minor peaks for dehydration of the Michael adducts of histidine. The ϵ-amino group of the lysyl residue is expected to be protonated. Bridging of a proton from this nitrogen to a hydroxyl

group can promote dehydration (see Scheme S2 in the Supporting Information). In contrast, loss of a hydroxyl group from the Michael adducts of histidine cannot be promoted by hydrogen bonding with the protonated imidazole. The MS/MS of 3:1 adduct at *m*/*z* 728, 732, 736, and 740 shows the presence of water loss at *m*/*z* 710, 714, 718, and 722 and *m*/*z* 692, 696, 700, and 704. Similarly, the peaks generated by loss of water by McLafferty rearrangement products **18**, **19**, **20**, **21**, and **22** of **17** are more intense than the peaks directly from McLafferty rearrangement (see the Supporting Information, Figure S9).

The product mixture from reaction of HNE (d_4:d_0, 1:1) with *N*-acetyl-Gly-Lys-OMe was separated by HPLC using a methanol/water gradient, and the molecular ions (discussed above) were monitored by LC-ESI/SIM/MS through 17 channels (see the Supporting Information, Figure S10). The chromatograms of adducts that differ only by the isotope content in the adducted HNE (d_0 or d_4) had similar features (retention times of peaks). Also, the complexity of the chromatogram peaks increases with increasing complexity of the adducts formed.

HNE Adducts of *N*-Acetyl-cysteine. ESI-TOF-MS analysis of a reaction between *N*-acetyl-cysteine and HNE (d_4:d_0, 1:1) in PBS buffer at 37 °C for 24 h revealed the presence of several multiple ion sets. The fragmentation of *N*-acetyl-cysteine was obtained as reported earlier (*38*). Cysteine forms a dimer under oxidative conditions through a disulfide bond (*39*). The molecular ion at *m*/*z* 325, corresponding to the dimer of *N*-acetyl-cysteine, generated daughter ions at *m*/*z* 307, 285, and 208 (see the Supporting Information, Figure S11). The Michael adducts of *N*-acetyl-cysteine with HNE (d_0:d_4, 1:1) have calculated molecular masses of *m*/*z* 320 and *m*/*z* 324. Because both the *N*-acetyl-cysteine dimer and the isotope-labeled (*N*-acetyl-cysteine)-HNE Michael adduct have the same *m*/*z*, the MS/MS spectra of (*N*-acetyl-cysteine)-HNE adduct ions are complicated. However, the ions that correspond to the loss of water, that is, *m*/*z* 302 and *m*/*z* 306, exhibit fragmentations without any interference (see the Supporting Information, Figure S12). As for the *N*-acetylhistidine Michael adduct of HNE, daughter ions at *m*/*z* 139 and 143 correspond to the HNE moiety derived from retro Michael cleavage of the adduct after loss of a molecule of water. Similar fragmentation of a cysteine-HNE Michael adduct was reported earlier using a deuterated cysteine (*40*).

The ESI-TOF-MS of the product mixture from the reaction of HNE with *N*-acetyl-cysteine (Figure 5B) shows many peaks that have the signature "multiplet" ions with *m*/*z* increments of 4 Da. The tandem MS/MS of these ions was recorded. The doublet of ions at *m*/*z* 465 and 469 (Figure 5B) corresponds to a cross-link between two molecules of *N*-acetyl-cysteine and one of HNE (see the Supporting Information, Figure S13 and Scheme S5). A "triplet" in the TIC at *m*/*z* 603, 607, and 611 (Figure 5B) corresponds to a cross-link formed between two molecules of *N*-acetyl-cysteine and two molecules of HNE in conjunction with loss two molecules of water (see the Supporting Information, Figure S14 and Scheme S6). Because only a small number of MS/MS fragment ions were detected, unambiguous structure assignments for these adducts must await further studies.

LC-ESI/SIM/MS analysis of the product mixture from the reaction of HNE with *N*-acetyl-cysteine was selectively monitored for most of the peaks that appear in the ESI-TOF-MS. The ESI chromatogram shown in Figure 5B represents the channels that have similar peak features for molecular ion sets corresponding to an adduct (MH^+) and its deuterium-labeled isomer(s) ($MH^+ + 4$ and/or $MH^+ + 8$). For example, molecular ions at *m*/*z* 603, 607, and 611 have peaks with the same features; however, for the parent ions *m*/*z* 320 and 324 [(*N*-acetyl-cysteine)-HNE Michael adduct], the peak features are different. This difference may be due to interference from molecular ions corresponding to (*N*-acetyl-cysteine)-(*N*-acetyl-cysteine) dimer that also have *m*/*z* 324. So, the Michael adduct is monitored as the MNa^+ ion at *m*/*z* 342 and 346 (see the Supporting Information, Figure S15).

Discussion

Lysine is an abundant amino acid (350 per LDL) in LDL. Lysine residues play a critical role in the function of apoB-100 and are the major targets of oxidative modifications. "Reactive" or available lysines in LDL are important for LDL binding to the LDL receptor (*41*) and the scavenger receptor (*42*) and for LDL modification. NMR spectroscopy of ^{13}C-labeled LDL was previously used to characterize the lysine residues in apoB-100. Reductive methylation with [^{13}C]formaldehyde converts up to two-thirds of the total lysines to their dimethylamino derivatives. This corresponds to 225 reactive lysines per LDL particle, which includes 53 "active" lysines with p*K* 8.9 and 172 "normal" lysines with p*K* 10.5 that are exposed on the surface of LDL. Another 132 lysines in the apoB-100 molecule are buried and unavailable (*41*). The TNBS assay is widely employed to determine the number of "active" lysine residues in LDL. Thus, 317 ± 29 reactive amino groups were detected in native LDL by TNBS assay (*43*).

It must be recognized that the number of reactive amino groups in LDL determined by TNBS assay would also include EPs because they can also react rapidly with TNBS to form the trinitrophenyl-EP chromophore that has $\lambda_{max} = 337$ nm. TNBS has been widely used as a nonpenetrating chemical probe to identify amino phospholipids located on the external surface of cells because of its rapid covalent binding to phosphatidyl ethanolamine (PE) (*44, 45*). The time course of the reaction of high-density lipoproteins (HDL) with TNBS shows two plateaus: One occurs after 60−90 min of incubation, and the other occurs at 15 h. It was presumed that TNBS reacts selectively with accessible lysine residues on the surface of HDL accounting for the first phase reaction (*46*). The second phase of the TNBS reaction was presumed to involve less "reactive" amino residues in HDL. The reaction of TNBS with amino phospholipids arranged as a monolayer on the surface of the HDL reached a plateau in only 10−20 min. There is no similar study on LDL. However, it is known that PE is depleted by 84% (determined by quantitative HPLC) in mildly oxidized LDL (*30*). Clearly, the modification of EP significantly contributes to the total amino residue modification of LDL. There are as many as 80 EPs per LDL, mainly PE (40%) and plasmenyl ethanolamine (60%).

ApoB-100, the protein component of LDL, is a hydrophobic protein, consisting of a single large polypeptide chain of 4536 amino acid residues with a molecular mass of 512 kDa. Unlike HSA, apoB-100 interacts with the phospholipid shell of LDL in such a way as to "organize" the surface monolayer (*47*). The lipid−protein interaction might have important consequences for the oxidation and modification behavior of LDL, and the mechanism by which LDL is oxidized and modified (*48*). Considering the total number of nucleophilic amino acid residues (350 Lys, 115 His, and 25 Cys) plus 80 EP (*41*) that might covalently react with HNE in LDL, the amount of HNE that can form adducts with LDL, for example, 486 molecules of per particle (Figure 3), is very high. This finding supports the view that HNE modification of LDL is a complex process, involving not only nucleophilic amino acid residues but also

Table 1. Nucleophilic Functional Groups in LDL

residue	total	reactive
lysine ϵ-NH_2	350	225[a]
EPs	80	80
histidine	115	115 (maximum)
cysteine	25	25 (maximum)
total	570	445

[a] TNBS reactive amino groups are 317 ± 29 and include all "reactive" (toward both TNBS and formaldehyde) lysines and all EPs or approximately 225 + 80 = 305. Maximum possible values are indicated since the number of "reactive" histidine and cysteine residues is unknown (*41*).

EPs. Although it is generally known that lysine ϵ-amino groups are major targets of HNE binding, it is also capable of modifying amino phospholipids in LDL (*49*). In fact, our TNBS studies of LDL primary amino group modification showed that only 165−230 of total 350 lysines plus 80 EPs were modified. The high estimate agrees well with the 225 reactive lysines detected by reductive methylation. Uchida et al. (*50*) found that 50 histidines and 40 lysines were "lost" per LDL, determined by amino acid analysis after reductive stabilization of HNE adducts by treatment with $NaBH_4$ and protein hydrolysis with 6 N HCl, upon the incubation of LDL (1.0 g/mL) with HNE (1.0 mM) for 2 h at 37 °C (*30, 50*). On the basis of these observations, it seems likely that most histidines would be modified upon treating LDL (0.5 mg/mL) with HNE (2 mM) for 48 h at 37 °C. Nevertheless, even assuming that all histidines and all cysteines are reactive, at least 41 of a total 486 HNE bound cannot be accounted for assuming only 1:1 adducts with all "reactive" lysyl residues, all EPs, histidine,and cysteine residues (Table 1). This suggests that some adducts can be generated that incorporate more than one HNE molecule. This conclusion is consistent with earlier model studies showing that the reaction of HNE with equimolar quantities of primary amines generates adducts that incorporate two (or more) equivalents of aldehyde per amine molecule (*16*). However, it should be noted that the amounts of HNE used in these studies are not typical of the amounts that are generated in vivo. Nevertheless, such high concentrations may be present in certain microdomains.

Adducts that incorporate multiple HNE molecules have not been previously structurally characterized. Perhaps such adducts are formed, but their lability confounds detection. We used mass spectrometry in conjunction with isotope labeling to facilitate structural characterization of these adducts. d_4-HNE, with deuterium in the inert C8 and C9 positions, was considered optimal for this purpose and was synthesized for these studies. The reaction of HNE (d_4:d_0, 1:1) with α-*N*-acyl amino acids generates products with "multiplet" (see the Supporting Information, pp S2−S4, for an explanation of this concept) peaks in the mass spectrum that are characteristic of the number of HNE molecules present in a particular adduct. This approach provides an analytical tool for identification of adducts that are labile under harsh conditions and/or present in low abundance.

The 1:1 adducts that were described previously (*51*) were characterized by MS/MS as reference standards for deciphering the fragmentation patterns of previously unknown adducts. By examining the reaction of *N*-acetyl histidine with a 1:1 mixture of HNE and d_4-HNE and structural characterization using a mass spectrometer, we detected adducts that correspond to multiple HNE adducted *N*-acetyl histidines. Similar multiple adducts were also detected using *N*-acetyl-glycine lysine methyl ester and *N*-acetyl cysteine. These results corroborate the conclusion of quantitative experiments using tritium-labeled HNE that showed a greater than 1:1 stoichiometric capacity of LDL to bind HNE.

Scheme 4. Domino-Like Multiple Michael Adduction of HNE with *N*-Acetyl-histidine

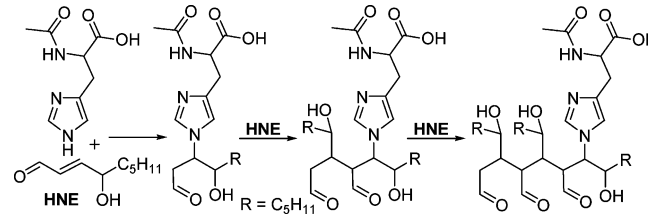

In addition to the quantitative conclusions enabled by the use of tritium-labeled HNE, the deuterium-labeled HNE experiments allowed a relative quantification of various adducts that are formed from lysine, cysteine, and histidine. Ion chromatograms were obtained by monitoring the masses corresponding to various adducts, and the areas of peaks corresponding to each adduct were measured using MassLynx software. For *N*-acetyl-lysine-glycine methyl ester, the relative amount of 2:1 and 3:1 HNE/*N*-acetyl-Gly-Lys-OMe adducts was about 18%. The 1:1 adducts (Michael, Schiff base, and pyrrole adduct) accounted for about 78% of the total and the 1:2 cross-link comprised about 1% of the total adducts monitored (Figure 9). In the case of *N*-acetyl histidine, the 1:1 Michael adduct accounts for about 70% of the adducts monitored, while the 2:1 and 3:1 HNE/*N*-acetyl-His adducts account for 25 and 6%, respectively (Figure 9). In the case of *N*-acetyl cysteine, the 1:1 Michael adduct (∼50%) was the predominant product, while 1:2 and 2:2 adducts were also major products, that is, ∼30 and ∼5%, respectively (Figure 9).

Conclusions

Using tritium-labeled HNE to quantitate the amount of HNE that binds with LDL, we showed that more HNE binds than can be accounted for by 1:1 adduction with all of the nucleophilic protein residues and amino phospholipids. In a model study, we detected and characterized the formation of 2:1 and 3:1 adducts of HNE with histidyl and lysyl nucleophiles using a 1:1 mixture of deuterium-labeled HNE and unlabeled HNE. Adducts formed with HNE give rise to apparent "multiplets" that are indicative of the number of HNE moieties present in each adduct. The tandem mass spectra of each of the adducts gave sets of unique daughter ions. This method is valuable for detecting and characterizing different types of adducts that are formed under mild conditions, including some present in low abundances. In addition to adduct types reported earlier from the reactions of lysine or histidine with HNE, the present studies with isotope-labeled HNE revealed adducts that incorporate multiple HNE molecules adducted with a single lysine or histidine residue. Our structural characterization of these adducts revealed that they are products of domino-like reactions of initial 1:1 HNE Michael adducts of histidyl (Scheme 4) or lysyl nucleophiles with multiple additional HNE molecules to form 2:1 and 3:1 adducts.

Although high concentrations of HNE might only be possible in certain microdomains in situ, for example, oxidized LDL particles, identification of such multiple HNE adducts may help in attaining a complete understanding of HNE's role in physiological processes. Furthermore, LDL can act as a magnet that attracts multiple molecules of HNE over time. The multiple HNE-amine adducts discussed here may constitute an initial response of proteins toward high levels of HNE. These multiple HNE adducts may rearrange to form other toxic products, or by corollary, this could be one of the in vivo homeostatic

mechanisms to detoxify lipid oxidation products by effectively quenching HNE's reactivity.

Acknowledgment. This work was supported by National Institutes of Health Grants HL53315 (R.G.S.), GM 21249 (R.G.S.), and EY 014239 (J.W.C.), a Foundation Fighting Blindness Research to Prevent Blindness Challenge Grant and Senior Investigator Award (J.W.C.), a Steinbach Award (J.W.C.), and an Ohio BRTT Award 05-29 (J.W.C. and R.G.S.). We also thank Dr. Stanley Hazen at the mass spectrometry core facility II at the Cleveland Clinic Foundation.

Supporting Information Available: Details of methods used for quantification and a discussion of the logic of our MS structural analysis with isotopologues of HNE (Figures S1−S15 and Schemes S1−S6) as well as NMR spectral data of new compounds (Figures S16−S20). This material is available free of charge via the Internet at http://pubs.acs.org.

References

(1) Mlakar, A., and Spiteller, G. (1996) Previously unknown aldehydic lipid peroxidation compounds of arachidonic acid. *Chem. Phys. Lipids 79*, 47–53.
(2) Harrison, K. A., and Murphy, R. C. (1995) Isoleukotrienes are biologically active free radical products of lipid peroxidation. *J. Biol. Chem. 270*, 17273–17278.
(3) Brown, M. S., and Goldstein, J. L. (1983) Lipoprotein metabolism in the macrophage: implications for cholesterol deposition in atherosclerosis. *Annu. Rev. Biochem. 52*, 223–261.
(4) Sun, M., and Salomon, R. G. (2004) Oxidative fragmentation of hydroxy octadecadienoates generates biologically active gamma-hydroxyalkenals. *J. Am. Chem. Soc. 126*, 5699–5708.
(5) Sun, M., Finnemann, S. C., Febbraio, M., Shan, L., Annangudi, S. P., Podrez, E. A., Hoppe, G., Darrow, R., Organisciak, D. T., Salomon, R. G., Silverstein, R. L., and Hazen, S. L. (2006) Light-induced oxidation of photoreceptor outer segment phospholipids generates ligands for CD36-mediated phagocytosis by retinal pigment epithelium: a potential mechanism for modulating outer segment phagocytosis under oxidant stress conditions. *J. Biol. Chem. 281*, 4222–4230.
(6) Poli, G., and Schaur, R. J. (2000) 4-Hydroxynonenal in the pathomechanisms of oxidative stress. *IUBMB Life 50*, 315–321.
(7) Uchida, K. (2003) 4-Hydroxy-2-nonenal: A product and mediator of oxidative stress. *Prog. Lipid Res. 42*, 318–343.
(8) Salomon, R. G., Kaur, K., Podrez, E., Hoff, H. F., Krushinsky, A. V., and Sayre, L. M. (2000) HNE-derived 2-pentylpyrroles are generated during oxidation of LDL, are more prevalent in blood plasma from patients with renal disease or atherosclerosis, and are present in atherosclerotic plaques. *Chem. Res. Toxicol. 13*, 557–564.
(9) Sayre, L. M., Zelasko, D. A., Harris, P. L., Perry, G., Salomon, R. G., and Smith, M. A. (1997) 4-Hydroxynonenal-derived advanced lipid peroxidation end products are increased in Alzheimer's disease. *J. Neurochem. 68*, 2092–2097.
(10) Macdonald, S., Dowle, M., Harrison, L., Clarke, G., Inglis, G., Johnson, M., Shah, P., Smith, R., Amour, A., Fleetwood, G., Humphreys, D., Molloy, C., Dixon, M., Godward, R., Wonacott, A., Singh, O., Hodgson, S., and Hardy, G. (2002) Discovery of further pyrrolidine trans-lactams as inhibitors of human neutrophil elastase (HNE) with potential as development candidates and the crystal structure of HNE complexed with an inhibitor (GW475151). *J. Med. Chem. 45*, 3878–3890.
(11) Szweda, L. I., Uchida, K., Tsai, L., and Stadtman, E. R. (1993) Inactivation of glucose-6-phosphate dehydrogenase by 4-hydroxy-2-nonenal. Selective modification of an active-site lysine. *J. Biol. Chem. 268*, 3342–3347.
(12) Crabb, J. W., O'Neil, J., Miyagi, M., West, K., and Hoff, H. F. (2002) Hydroxynonenal inactivates cathepsin B by forming Michael adducts with active site residues. *Protein Sci. 11*, 831–840.
(13) Isom, A. L., Barnes, S., Wilson, L., Kirk, M., Coward, L., and Darley-Usmar, V. (2004) Modification of Cytochrome c by 4-hydroxy-2-nonenal: Evidence for histidine, lysine, and arginine-aldehyde adducts. *J. Am. Soc. Mass. Spectrom. 15*, 1136–1147.
(14) Doorn, J. A., and Petersen, D. R. (2003) Covalent adduction of nucleophilic amino acids by 4-hydroxynonenal and 4-oxononenal. *Chem.-Biol. Interact. 143−144*, 93–100.
(15) Nadkarni, D. V., and Sayre, L. M. (1995) Structural definition of early lysine and histidine adduction chemistry of 4-hydroxynonenal. *Chem. Res. Toxicol. 8*, 284–291.
(16) Sayre, L. M., Arora, P. K., Iyer, R. S., and Salomon, R. G. (1993) Pyrrole formation from 4-hydroxynonenal and primary amines. *Chem. Res. Toxicol. 6*, 19–22.
(17) Jurgens, G., Lang, J., and Esterbauer, H. (1986) Modification of human low-density lipoprotein by the lipid peroxidation product 4-hydroxynonenal. *Biochim. Biophys. Acta 875*, 103–114.
(18) Bubnis, W. A., and Ofner, C. M., 3rd (1992) The determination of epsilon-amino groups in soluble and poorly soluble proteinaceous materials by a spectrophotometric method using trinitrobenzenesulfonic acid. *Anal. Biochem. 207*, 129–133.
(19) Deng, Y., and Salomon, R. G. (1998) Synthesis of [9-3H]-*trans*-4-Hydroxy-2-nonenal. *J. Org. Chem. 63*, 3504–3507.
(20) Kamido, H., Kuksis, A., Marai, L., and Myher, J. J. (1992) Identification of cholesterol-bound aldehydes in copper-oxidized low density lipoprotein. *FEBS Lett. 304*, 269–272.
(21) Kates, M. (1986) *Techniques of Lipidology: Isolation, Analysis, and Identification of Lipids*, 2nd rev. ed., Elsevier, Amsterdam, The Netherlands.
(22) Edwards, G. L., Muldoon, C. A., and Sinclair, D. J. (1996) Cyclic enol ether synthesis via arenesulfonyl iodide additions to alkynols. *Tetrahedron 52*, 7779–7788.
(23) Birch, A. J., and Walker, K. A. M. (1966) *J. Chem. Soc. C* 1894.
(24) Felder, S., and Rowan, D. D. (1999) Synthesis of deuterated C-6 and C-9 flavour volatiles. *J. Labelled Compd. Radiopharm. 42*, 83–92.
(25) Deng, Y., and Salomon, R. G. (2002) Synthesis of [9-^{3}H]-*trans*-4-Hydroxy-2-nonenal. *J. Org. Chem. 63*, 3504–3507.
(26) Esterbauer, H., Schaur, R. J., and Zollner, H. (1991) Chemistry and biochemistry of 4-hydroxynonenal, malonaldehyde and related aldehydes. *Free Radical Biol. Med. 11*, 81–128.
(27) Fields, R. (1971) The measurement of amino groups in proteins and peptides. *Biochem. J. 124*, 581–590.
(28) Bubnis, W. A., and Ofner, C. M., 3rd (1992) The determination of epsilon-amino groups in soluble and poorly soluble proteinaceous materials by a spectrophotometric method using trinitrobenzenesulfonic acid. *Anal. Biochem. 207*, 129–133.
(29) Steinbrecher, U. P. (1987) Oxidation of human low density lipoprotein results in derivatization of lysine residues of apolipoprotein B by lipid peroxide decomposition products. *J. Biol. Chem. 262*, 3603–3608.
(30) Sevanian, A., Bittolo-Bon, G., Cazzolato, G., Hodis, H., Hwang, J., Zamburlini, A., Maiorino, M., and Ursini, F. (1997) LDL- is a lipid hydroperoxide-enriched circulating lipoprotein. *J. Lipid. Res. 38*, 419–428.
(31) Amarnath, V., Valentine, W. M., Montine, T. J., Patterson, W. H., Amarnath, K., Bassett, C. N., and Graham, D. G. (1998) Reactions of 4-hydroxy-2(*E*)-nonenal and related aldehydes with proteins studied by carbon-13 nuclear magnetic resonance spectroscopy. *Chem. Res. Toxicol. 11*, 317–328.
(32) Deng, Y. (2000) *Oxidized Lipids: Part I: Radiochemical Studies on HNE-Protein Adduction Part II: Total Synthesis of Oxidized Phospholipids and Cholesterol Esters*, Department of Chemistry, Case Western Reserve University, Cleveland, OH.
(33) Enoiu, M., Herber, R., Wennig, R., Marson, C., Bodaud, H., Leroy, P., Mitrea, N., Siest, G., and Wellman, M. (2002) gamma-Glutamyltranspeptidase-dependent metabolism of 4-hydroxynonenal-glutathione conjugate. *Arch. Biochem. Biophys. 397*, 18–27.
(34) Gioacchini, A. M., Calonghi, N., Boga, C., Cappadone, C., Masotti, L., Roda, A., and Traldi, P. (1999) Determination of 4-hydroxy-2-nonenal at cellular levels by means of electrospray mass spectrometry. *Rapid Commun. Mass Spectrom. 13*, 1573–1579.
(35) Aldini, G., Granata, P., and Carini, M. (2002) Detoxification of cytotoxic alpha,beta-unsaturated aldehydes by carnosine: Characterization of conjugated adducts by electrospray ionization tandem mass spectrometry and detection by liquid chromatography/mass spectrometry in rat skeletal muscle. *J. Mass Spectrom. 37*, 1219–1228.
(36) Fenaille, F., Guy, P. A., and Tabet, J.-C. (2003) Study of protein modification by 4-hydroxy-2-nonenal and other short chain aldehydes analyzed by electrospray ionization tandem mass spectrometry. *J. Am. Soc. Mass Spectrom. 14*, 215–226.
(37) SDBS. http://www.aist.go.jp/RIODB/SDBS/ (National Institute of Advanced Industrial Science and Technology), 2005.
(38) Steen, H., and Mann, M. (2001) Similarity between condensed phase and gas phase chemistry: Fragmentation of peptides containing oxidized cysteine residues and its implications for proteomics. *J. Am. Soc. Mass Spectrom. 12*, 228–232.
(39) Doreleijers, J. F. (1999) *Validation of Biomolecular NMR Structures*, Universiteit Utrecht, Utrecht, The Netherlands; http://tang.bmrb.wisc.edu/~jurgen/Thesis/Thesis.pdf.
(40) Rathahao, E., Peiro, G., Martins, N., Alary, J., Gueraud, F., and Debrauwer, L. (2005) Liquid chromatography-multistage tandem mass spectrometry for the quantification of dihydroxynonene mercapturic acid (DHN-MA), a urinary end-metabolite of 4-hydroxynonenal. *Anal. Bioanal. Chem. 381*, 1532–1539.

(41) Lund-Katz, S., Ibdah, J. A., Letizia, J. Y., Thomas, M. T., and Phillips, M. C. (1988) A 13C NMR characterization of lysine residues in apolipoprotein B and their role in binding to the low density lipoprotein receptor. *J. Biol. Chem. 263*, 13831–13838.
(42) Zhang, H., Yang, Y., and Steinbrecher, U. (1993) Structural requirements for the binding of modified proteins to the scavenger receptor of macrophages. *J. Biol. Chem. 268*, 5535–5542.
(43) Bermejo, P., Gomez-Serranillos, P., Santos, J., Pastor, E., Gil, P., and Martin-Aragon, S. (1997) Determination of malonaldehyde in Alzheimer's disease: a comparative study of high-performance liquid chromatography and thiobarbituric acid test. *Gerontology 43*, 218–222.
(44) Sanchez-Yague, J., and Llanillo, M. (1986) Lipid composition of subcellular particles from sheep platelets. Location of phosphatidylethanolamine and phosphatidylserine in plasma membranes and platelet liposomes. *Biochim. Biophys. Acta 856*, 193–201.
(45) Chiu, D., Lubin, B., and Shohet, S. B. (1979) Erythrocyte membrane lipid reorganization during the sickling process. *Br. J. Haematol. 41*, 223–234.
(46) Tsuchihashi, K., and Minari, O. (1983) Lysine residues located on the surface of human plasma high-density lipoprotein particles. *Biochim. Biophys. Acta 752*, 10–18.
(47) Loidl-Stahlhofen, A., Hannemann, K., and Spiteller, G. (1994) Generation of alpha-hydroxyaldehydic compounds in the course of lipid peroxidation. *Biochim. Biophys. Acta 1213*, 140–148.
(48) Carmen Vigo-Pelfrey, E. (1990) *Membrane Lipid Oxidation*, Vol. I, CRC Press, Menlo Park, CA.
(49) Guichardant, M., Taibi-Tronche, P., Fay, L. B., and Lagarde, M. (1998) Covalent modifications of aminophospholipids by 4-hydroxynonenal. *Free Radical Biol. Med. 25*, 1049–1056.
(50) Uchida, K., Toyokuni, S., Nishikawa, K., Kawakishi, S., Oda, H., Hiai, H., and Stadtman, E. R. (1994) Michael addition-type 4-hydroxy-2-nonenal adducts in modified low-density lipoproteins: Markers for atherosclerosis. *Biochemistry 33*, 12487–12494.
(51) Uchida, K. (2003) Histidine and lysine as targets of oxidative modification. *Amino Acids 25*, 249–257.

TX8000303